DEVELOPMENT OF NONLOCAL GREEN-KUBO FORMALISM WITH APPLICATIONS TO COUPLED HEAT AND MASS TRANSPORT

by

KEVIN FERNANDO

A thesis submitted in partial fulfillment of the requirements
for the degree of Bachelor of Science
in the Department of Physics
in the College of Sciences
at the University of Central Florida
Orlando, Florida

Fall Term 2019

Thesis Chair: Dr. Patrick Schelling, Ph.D.

1 ABSTRACT

Nonlocal equations for coupled heat and mass transport are developed within the Green-Kubo formalism. Nonlocal thermal transport in Lennard-Jones solids is computed to establish the existence of semi-ballistic transport. Deviations from the diffusive theory are shown by comparing the Fourier transform of the response function from the nonlocal theory to that of the diffusive one. It is shown that the deviations from the local theory correspond to acoustic phonons, whose frequency dependence gives rise to the observed deviations from the local theory.

2 TABLE OF CONTENTS

3 LIST OF FIGURES

4 LIST OF TABLES

5 OBJECTIVES AND INTRODUCTION

Linear response theory assumes that response currents are linear in the driving forces. These driving forces come in the form of gradients of physical quantities. This can be evidenced by examining Fick's laws, or Fourier's law. In particular, Fick's first law states that the flux density, $\vec{J}$ is proportional to the gradient of the density, $\eta(\vec{r})$.

$$\vec{J} = -D\vec{\nabla}\eta(\vec{r}) \tag{1}$$

Here D is called the diffusion coefficient, and $\vec{\nabla}\eta(\vec{r})$ is the driving force. This equation can be combined with the continuity equation, which states that law of conservation of mass $\frac{\partial\eta(\vec{r})}{\partial t} = -\vec{\nabla}\cdot\vec{J}(\vec{r})$, to get Fick's Second Law, $\frac{\partial\eta(\vec{r})}{\partial t} = D\nabla^2\eta(\vec{r})$. The other relevant law, Fourier's law, states that the current $\vec{J}(\vec{r})$ is proportional to a temperature gradient, $\vec{J}(\vec{r}) = -\kappa\vec{\nabla}T(\vec{r})$. Here κ is the thermal conductivity, and T is the temperature.

Note that the aforementioned laws are all local. By that we mean they depend only on $\vec{r}$ the point at which the response is being evaluated. This is in contrast to, for example, electrical conduction which is considered as a nonlocal effect. Here the object of interest is electrical conductivity, $\sigma(\vec{r},\vec{r'})$ which when an external electric field, $\vec{E}$, is applied relates to the current density, $\vec{J}(\vec{r})$, by

$$\vec{J}(\vec{r}) = \int \sigma(\vec{r},\vec{r'})\vec{E}(\vec{r})d^3x \tag{2}$$

Here σ is a second rank tensor. A similar equation can be written down for thermal conductivity. The response is given by

$$\vec{J}(\vec{r}) = \int \kappa(\vec{r},\vec{r'})\vec{\nabla}T(\vec{r})d^3x \tag{3}$$

Where κ is a second rank tensor, and T is a temperature field. Note that σ and κ also depend on other points $\vec{r'}$, which characterize the above equations as nonlocal.

While the local formalism has been sufficient for many applications in heat transport, it

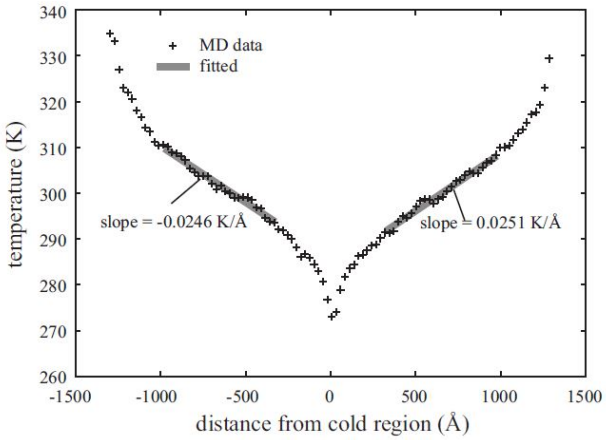

Figure 1: Distance vs. temperature graph displays the violating of Fourier's law, indicating a nonlocal treatment is required to fully model the data.

has recently been shown that when temperature gradients are imposed for small systems Fourier's law breaks down. For example in Fig. 1 an MD simulation by Zhou *et al.* [1] shows a nonlinear temperature gradient indicating partially ballistic transport and nonlocal behavior. This issue was then investigated by Allen [2] who analyzed Eq. 3 in Fourier space by Fourier expanding the conductivity tensor. Theoretical fits were then made using solutions to the Boltzmann Transport equation (BTE), see Fig. 2.

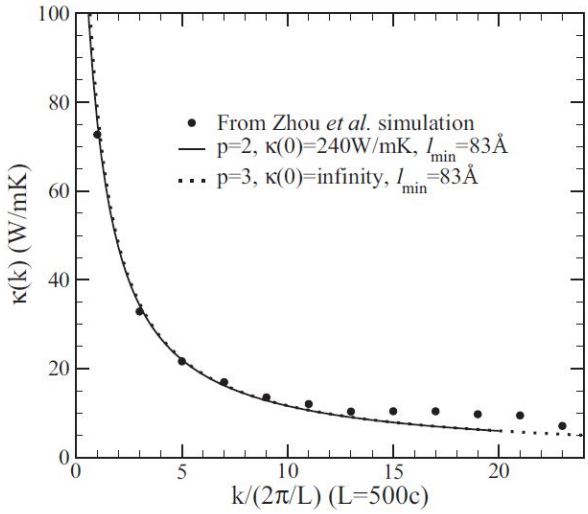

Figure 2: The bold dots represent the data by Zhou *etal.* [1], while P=2 and P=3 represent theoretical fits using a Debye Model RTA fit.

6 FLUCTUATION-DISSIPATION THEORY

In the Fluctuation-Dissipation Theorem, the basic idea is that the response to a system perturbed by an external driving force can be understood by examining the nature of fluctuations in equilibrium. There are several excellent examples of this in Brownian motion and drag as well as with Johnson noise and resistance. Specifically for Brownian motion, Einstein was one of the first to give a quantitative relation between random fluctuations and mobility in the presence of an external field, now known as the Einstein relation. Consider a system of particles with density $\eta(x)$ in the presence of a scalar potential field $V(x)$. The dissipative part of the response will be $J(x) = -\mu\frac{dV(x)}{dx}\eta(x)$ where μ is the mobility, and the total response will be [3],

$$J(x) = -D\frac{d\eta(x)}{dx} - \mu\frac{dV(x)}{dx}\eta(x) \tag{4}$$

If we allow this system to reach equilibrium $J \to 0$, and $\eta(x)$ will obey a Boltzmann distribution, $\eta(x) = \gamma e^{-V(x)\beta}$ where γ is a constant and $\beta = \frac{1}{k_B T}$. Substituting back into eq. 4 with $J = 0$ gives

$$0 = D\eta\frac{dV}{dx}\beta - \frac{dV}{dx}\eta\gamma \tag{5}$$

$$D = \mu k_B T \tag{6}$$

This fundamental result tells us that the physical mechanism which controls fluctuations in an equilibrium ensemble is the same as that which dictates dissipation effects. This was the first of many results which were generalized to be called the Fluctuation-Dissipation Theorem [3].

7 NONLOCAL RESPONSE FUNCTIONS

In his now famous paper, Kubo [4] was able to show that the Fluctuation Dissipation Theorem can be used to compute transport coefficients, including the thermal conductivity. The equations were derived under the assumption of linear response in the driving force, and were a completely local formulation. These equations became known as the Green-Kubo (GK) relations and are still widely used today.

In heat conduction, generally a local formulation using Fourier's law is applied. Thermal conductivity can be found from the GK relations [5]

$$\kappa_{\mu\nu} = \frac{1}{\Omega k_B T^2} \int_0^\infty < J_\mu(\tau) J_\nu(0) > d\tau \tag{7}$$

Here $\kappa_{\mu\nu}$ is the thermal conductivity tensor, J_μ is the heat flux density, Ω is the system volume, k_B is the Boltzmann constant, and T is the temperature. The angle brackets signify an equilibrium ensemble average and the quantity $< J_\mu(\tau) J_\nu(0) >$ is the current-current autocorrelation function. Hence the fluctuations in equilibrium are connected with the dissipation via the thermal conductivity. Note that Eq. 7 is established by assuming diffusive transport and that Fourier's law holds.

Many practical applications in nanoscale materials involve partially ballistic transport, where heat carriers (e.g. the phonons) propagate over distances comparable to the dimensions of the material. For example, experiments of semiconductor alloys [6] reported thermal conductivities which depend on the frequency of the oscillating temperature field used in the measurement. In order to theoretically understand transport in the diffuse/ballistic limit a nonlocal approach is required. We now begin developing such a formalism.

We aim to establish a nonlocal approach to transport, and expect the nonlocal theory to give a result which goes beyond Eq. 7. We begin by considering a general nonlocal form with response function $K_{\mu\nu}(\vec{x} - \vec{x}', t - t')$, which relates the heat flux density to the external

heat sources and sinks,

$$J_\mu(\vec{x},t) = -\left(\frac{1}{3k_B}\right)\int_\Omega\int_{-\infty}^{t}\sum_\nu K_{\mu\nu}(\vec{x}-\vec{x}',t-t')\frac{\partial^2\Delta u^{(ext)}(\vec{x}',t')}{\partial t'\partial x'_\nu}d^3x'dt' \tag{8}$$

where $\Delta u^{(ext)}(\vec{x}',t')$ represents energy density added or removed locally near $\vec{x}'$. This expression takes into account the finite propagation time for the heat pulse, and hence an important limitation on ballistic transport. While this expression is suitable for time-dependent heat sources and sinks, it can also be applied to static nonequilibrium situations. Hence this is compatible with the expression in Eq. [2], but goes somewhat beyond it to time-dependent situations which would be relevant to many experiments including pulsed laser heating or the response of materials to high-frequency heating via electron-phonon scattering in semiconductor devices.

We develop an approach to use Green-Kubo calculations to determine the nonlocal response function $K_{\mu\nu}(\vec{x}-\vec{x}',t-t')$, which is then applied to transport in a solid Ar system. We begin by expanding the current,

$$J_\mu(\vec{x},t) = \tilde{J}_\mu(0,t) + \sum_{\vec{k}\neq 0}\tilde{J}_\mu(\vec{k},t)e^{i\vec{k}\cdot\vec{x}} \tag{9}$$

Similarly, the energy density can be expanded in a Fourier series,

$$\Delta u^{(ext)}(\vec{x}',t') = \sum_{\vec{k}\neq 0}\tilde{u}^{(ext)}(\vec{k},t')e^{i\vec{k}\cdot\vec{x}'} \tag{10}$$

in which we have made the assumption that the net input energy is zero, hence $\tilde{u}(\vec{k}=0,t') = 0$ at all times. The response function is similarly expanded, with the assumption that the system in question is isotropic,

$$K_{\mu\nu}(\vec{x}-\vec{x}',t-t') = \tilde{K}_{\mu\nu}(0,t) + \sum_{\vec{k}\neq 0}\tilde{K}_{\mu\nu}(\vec{k},t)e^{i\vec{k}\cdot(\vec{x}-\vec{x}')} \tag{11}$$

Substitution of these expressions into Eq. 8 yields,

$$\tilde{J}_\mu(\vec{k},t) = -i\left(\frac{\Omega}{3k_B}\right)\sum_\nu \int_{-\infty}^{t} k_\nu \tilde{K}_{\mu\nu}(\vec{k},t-t')\frac{\partial \tilde{u}^{(ext)}(\vec{k},t')}{\partial t'}dt' \tag{12}$$

To obtain an expression which can be used to evaluate the response functions, we consider an external source,

$$\frac{\partial \tilde{u}^{(ext)}(\vec{k},t')}{\partial t'} = \tilde{u}^{(ext)}(\vec{k})\delta(t') \tag{13}$$

in which $\delta(t')$ is the Dirac delta function. Using Eq. 13 the integral in Eq. 12 can be evaluated,

$$\tilde{J}_\mu(\vec{k},t) = -i\left(\frac{\Omega}{3k_B}\right)\sum_\nu k_\nu \tilde{K}_{\mu\nu}(\vec{k},t)\tilde{u}^{(ext)}(\vec{k}) \tag{14}$$

This expression determines the heat-flux density which results from an input energy.

To obtain the response function, we can develop a Green-Kubo expression starting from Eq. 14. First we assume that an external source $\tilde{u}^{(ext)}(\vec{k})$ can be equated to a fluctuation of a system in equilibrium $\tilde{u}(\vec{k})$. After this substitution, we multiply Eq. 14 by $ik_\mu\tilde{u}(-\vec{k})$, sum over each direction μ, and take an ensemble average,

$$\sum_\mu \langle ik_\mu \tilde{J}_\mu(\vec{k},\tau)\tilde{u}(-\vec{k})\rangle = -\left(\frac{\Omega}{3k_B}\right)\sum_\mu\sum_\nu k_\mu k_\nu \tilde{K}_{\mu\nu}(\vec{k},\tau)\langle\tilde{u}(\vec{k})\tilde{u}(-\vec{k})\rangle \tag{15}$$

where τ is the time relative to the fluctuation. Using the continuity equation and time-reversal symmetry, and finally taking a derivative with respect to τ, it can then be shown that the response function is given by,

$$\frac{\partial \tilde{K}_{\mu\nu}(\vec{k},\tau)}{\partial\tau} = -\left(\frac{3k_B}{\Omega}\right)\frac{\langle \tilde{J}_\mu(\vec{k},\tau)\tilde{J}_\nu(-\vec{k},0)\rangle}{\langle\tilde{u}(\vec{k})\tilde{u}(-\vec{k})\rangle} \tag{16}$$

Integration of this expression over the time variable τ results in,

$$\tilde{K}_{\mu\nu}(\vec{k},\tau) - \tilde{K}_{\mu\nu}(\vec{k},0) = -\left(\frac{3k_B}{\Omega}\right)\frac{\int_0^\tau \langle \tilde{J}_\mu(\vec{k},\tau')\tilde{J}_\nu(-\vec{k},0)\rangle d\tau'}{\langle\tilde{u}(\vec{k})\tilde{u}(-\vec{k})\rangle} \tag{17}$$

Taking the limit where $\tau \to \infty$ we obtain,

$$\tilde{K}_{\mu\nu}(\vec{k},0) = \left(\frac{3k_B}{\Omega}\right) \frac{\int_0^\infty \langle \tilde{J}_\mu(\vec{k},\tau)\tilde{J}_\nu(-\vec{k},0)\rangle d\tau}{\langle \tilde{u}(\vec{k})\tilde{u}(-\vec{k})\rangle} \tag{18}$$

Here we have used that $\lim_{\tau\to\infty} \tilde{K}_{\mu\nu}(\vec{k},\tau) = 0$. These can be combined to obtain another relationship, namely

$$\tilde{K}_{\mu\nu}(\vec{k},\tau) = \left(\frac{3k_B}{\Omega}\right) \frac{\int_\tau^\infty \langle \tilde{J}_\mu(\vec{k},\tau')\tilde{J}_\nu(-\vec{k},0)\rangle d\tau'}{\langle \tilde{u}(\vec{k})\tilde{u}(-\vec{k})\rangle} \tag{19}$$

We also see the connection between these results for finite $\vec{k}$ and the bulk thermal conductivity defined by the Fourier law and the GK expression, namely

$$\kappa_{\mu\nu} = \lim_{|\vec{k}|\to 0} \tilde{K}_{\mu\nu}(\vec{k},0) = \frac{\Omega}{k_B T^2} \int_0^\infty \lim_{|\vec{k}|\to 0} \langle \tilde{J}_\mu(\vec{k},\tau)\tilde{J}_\nu(-\vec{k},0)\rangle d\tau \tag{20}$$

in which we have used the fluctuation formula for the heat capacity and the classical equipartition theorem,

$$\langle \tilde{u}(\vec{k})\tilde{u}(-\vec{k})\rangle = \frac{3\left(k_B T\right)^2}{\Omega^2} \tag{21}$$

Furthermore, using this expression, we can write a concise expression for $\tilde{K}_{\mu\nu}(\vec{k},\tau)$,

$$\tilde{K}_{\mu\nu}(\vec{k},\tau) = \frac{\Omega}{k_B T^2} \left[\int_0^\infty \langle \tilde{J}_\mu(\vec{k},\tau)\tilde{J}_\nu(-\vec{k},0)\rangle d\tau - \int_0^\tau \langle \tilde{J}_\mu(\vec{k},\tau)\tilde{J}_\nu(-\vec{k},0)\rangle d\tau\right] \tag{22}$$

In the following we consider a system with cubic symmetry, such that

$$\tilde{K}_{\mu\nu}(\vec{k},\tau) = \tilde{K}(\vec{k},\tau)\delta_{\mu,\nu} \tag{23}$$

where $\delta_{\mu,\nu}$ is the Kroenecker delta function. In this case the current direction is exactly along the direction $\vec{k}$ corresponding to the external perturbation. Hence we can define,

$$\tilde{J}_\mu(\vec{k},\tau) = \tilde{J}(\vec{k},\tau)\frac{k_\mu}{k} \tag{24}$$

in which $k = |\vec{k}|$. Given these simplifications for a cubic system, it is then easy to show that

the response function only depends on the magnitude of $\vec{k}$. We obtain the expression,

$$\tilde{K}(k,\tau) = \frac{\Omega}{k_B T^2}\left[\int_0^\infty \langle \tilde{J}(\vec{k},\tau)\tilde{J}(-\vec{k},0)\rangle d\tau - \int_0^\tau \langle \tilde{J}(\vec{k},\tau)\tilde{J}(-\vec{k},0)\rangle d\tau\right] \tag{25}$$

There are many different vectors $\vec{k}$ with magnitude k. Hence, to obtain $\tilde{K}(k,\tau)$, we average over each direction. To compare to the Fourier theory, we consider Fourier transforms of the function $\tilde{K}(k,\tau)$,

$$D(\vec{k},\omega) = \int_0^\infty \tilde{K}(\vec{k},\tau)e^{-i\omega\tau}d\tau \tag{26}$$

.

This can be contrasted with the local Fourier theory. In the Fourier theory, an external heat pulse $\tilde{u}^{(ext)}(\vec{k},0)$ occurring at $t = 0$ in a system in equilibrium results in the response for later times,

$$\tilde{u}(\vec{k},\tau) = e^{-\alpha k^2 \tau}\tilde{u}^{(ext)}(\vec{k},0) \tag{27}$$

where we have assumed an isotropic system. The thermal diffusivity is given by $\alpha = \frac{\kappa}{c_V}$, where κ is the thermal conductivity and c_V is the volumetric specific heat capacity. In terms of the Fourier components of the current density, we obtain from the Fourier theory

$$\tilde{J}_\mu(\vec{k},\tau) = -ik_\mu\left(\frac{\kappa\Omega}{3k_B}\right)e^{-\alpha k^2\tau}\tilde{u}^{(ext)}(\vec{k},0) \tag{28}$$

Comparison to the nonlocal expressions above, this suggests we should consider the transform,

$$K_T(k,\omega) = \kappa\int_0^\infty e^{-\alpha k^2\tau}e^{-i\omega\tau}d\tau = \kappa\left[\frac{\alpha k^2 - i\omega}{(\alpha k^2)^2 + \omega^2}\right] \tag{29}$$

Differences between the nonlocal theory in Eq. 26 and the Fourier theory prediction in Eq. 29 represent ballistic transport processes. In the Fourier theory, if the external perturbation is given by,

$$\frac{\partial \Delta u^{(ext)}(\vec{x},t)}{dt} = \frac{1}{4}a\left(e^{i\omega t} + e^{-i\omega t}\right)\left(e^{i\vec{k}\cdot\vec{x}} + e^{-i\vec{k}\cdot\vec{x}}\right) = a\cos\left(\vec{k}\cdot\vec{x}\right)\cos\left(\omega t\right) \tag{30}$$

the resulting heat flux density is,

$$\vec{J}(\vec{x},t) = \vec{k}\left(\frac{a\Omega\kappa}{3k_B}\right)\frac{\alpha k^2\cos\omega t + \omega\sin\omega t}{(\alpha k^2)^2+\omega^2}\sin\left(\vec{k}\cdot\vec{x}\right) \tag{31}$$

This indicates that the current lags the input power in time. Specifically we can write,

$$\vec{J}(\vec{x},t) = \vec{k}\left(\frac{a\Omega\kappa}{3k_B}\right)\frac{\cos(\omega t-\delta)}{(\alpha k^2)^2+\omega^2}\sin\left(\vec{k}\cdot\vec{x}\right) \tag{32}$$

with the relative phase angle given by,

$$\tan\delta = \frac{\omega}{\alpha k^2} \tag{33}$$

Equating the above expression to the Fourier law also yields the temperature distribution,

$$T(\vec{x},t) = \left(\frac{a\Omega}{3k_B}\right)\frac{\cos(\omega t-\delta)}{(\alpha k^2)^2+\omega^2}\cos\left(\vec{k}\cdot\vec{x}\right) \tag{34}$$

Physically, one can see that if the driving frequency is very low, such that $\alpha k^2 \gg \omega$, that $\delta \to 0$, and the system follows the perturbation in time. However, if the frequency becomes very large, then $\delta \to \frac{\pi}{2}$.

In summary, the real part of $K_T(k,\omega)$ corresponds to the heat-flux density which is in-phase with the external input power, whereas the imaginary part of $K_T(k,\omega)$ relates to the tendency of the heat-flux density to lag the external input power. Another important observation which applies to $K_T(k,\omega)$ in both the nonlocal and Fourier theories is,

$$K_T^*(k,\omega) = K_T(k,-\omega) \tag{35}$$

8 APPROACH

The equations for nonlocal transport were used to analyze large systems of a single component solid noble gas using Moluecular Dynamics (MD) simulations. These are computer run simulations which model each atoms movement by numerically integrating Newton's 2nd law under the action of a Lennard-Jones (LJ) potential. This famous pair potential is a model for inter-atomic forces of noble gases.

Our simulation results were generated using Lennard-Jones potentials, with the interaction between particles given by,

$$\phi^0(r) = -4\epsilon \left[\left(\frac{\sigma}{r}\right)^6 - \left(\frac{\sigma}{r}\right)^{12} \right] \tag{36}$$

where r is the separation between the particles. To ensure computational efficiency, a cutoff of $r_c = 3\sigma$ was used, with σ always taken to be the size of the largest atom. For atom separations $r > r_c$, the interaction was taken to be zero. When $r < r_c$, to ensure no discontinuities in the potential or forces existed, the potentials were smoothed by calculating the interactions from the effective potential,

$$\phi(r_{ij}) = \phi^0(r_{ij}) - \phi^0(r = r_c) - (r - r_c) \left[\frac{d\phi}{dr} \right]_{r=r_c} \tag{37}$$

Because the cutoff $r_c = 3\sigma_{11}$ is large, the effect of smoothing is minimal. The leading discontinuity occurs in the second derivative at $r = r_c$.

In order to obtain a microscopic definition for the heat flux, it is necessary to define a local energy associated with each site. The local energy is chosen to be given by,

$$\epsilon_i = \frac{1}{2} m_i \vec{v}_i \cdot \vec{v}_i + \frac{1}{2} \sum_{j \neq i} \phi(r_{ij}) \tag{38}$$

In the following, the heat flux due to convective and virial contributions are separately

determined. For the convective heat flux,

$$\vec{J}^{(conv)} = \sum_{i=1}^{N_1} \epsilon_i \vec{v}_i \tag{39}$$

Likewise for the virial contribution,

$$\vec{J}^{(vir)} = -\frac{1}{2} \sum_{i=1}^{N_1} \vec{r_{ij}} \left[\frac{1}{r} \frac{d\phi}{dr} \right]_{r=r_{ij}} (\vec{r_{ij}} \cdot \vec{v}_i) \tag{40}$$

Then the net heat flux is given by the sum of the convective and virial contributions from the two components,

$$\vec{J} = \vec{J}^{(conv)} + \vec{J}^{(vir)} \tag{41}$$

9 RESULTS

MD runs were conducted for a single component (Ar) system containing 2048 atoms at $T = 10K, 20K, 30K, 40K, 50K, 60K$ in an fcc cubic lattice. Each simulation was run for 3×10^5 MD steps and averaged over 30 separate runs. The Ar system was ran with the following parameters for Ar: $\sigma = 0.340nm$, $\frac{\epsilon}{k_B} = 120K$, $m = 39.948amu$ We have tabulated other relevant input parameters in Tbl. 1, including the reduced density and reduced temperature $\rho* = \rho\sigma^3$, $T^* = \frac{T}{120K}$ respectively. Note that while our system parameters were slightly different, our thermal conductivity results align with that of Ref. [7].

Table 1: Parameters for MD simulations

ρ^*	T*	T [K]	κ $[\frac{W}{mK}]$
1.02	0.083	10	1.794
1.02	0.166	20	0.847
1.02	0.250	30	0.5576
1.02	0.333	40	0.4377
1.02	0.416	50	0.4234
1.02	0.500	60	0.3284

A sample run of $\kappa(\tau) = \frac{\Omega}{k_B T^2} \int_0^\tau \langle \tilde{J}(0,\tau)\tilde{J}(0,0)\rangle d\tau$ for 20K is shown in Fig.3 to demonstrate that convergence was achieved and the conductivity was recorded at 30 ps. Note how the error grows, as we look at longer time, the signal to noise ratio becomes worse, yielding increasing error-bars and at very long time could falsely show growth or decline in $\kappa(\tau)$.

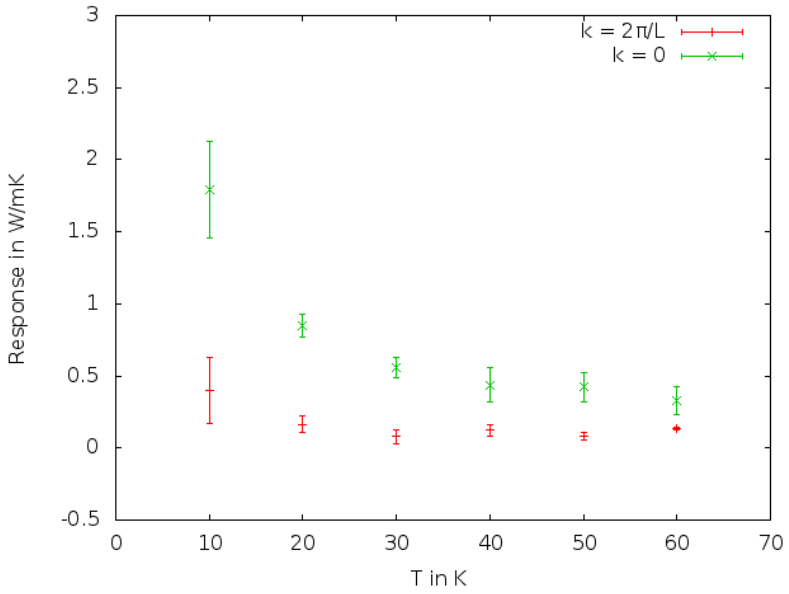

Figure 4: Plot displaying real part of $\left(\frac{\Omega}{k_B T^2}\right) \int_0^\infty \langle \tilde{J}(\vec{k},\tau)\tilde{J}(-\vec{k},0)\rangle d\tau$ for $k=0$, $k=\frac{2\pi}{L}$ at different T.

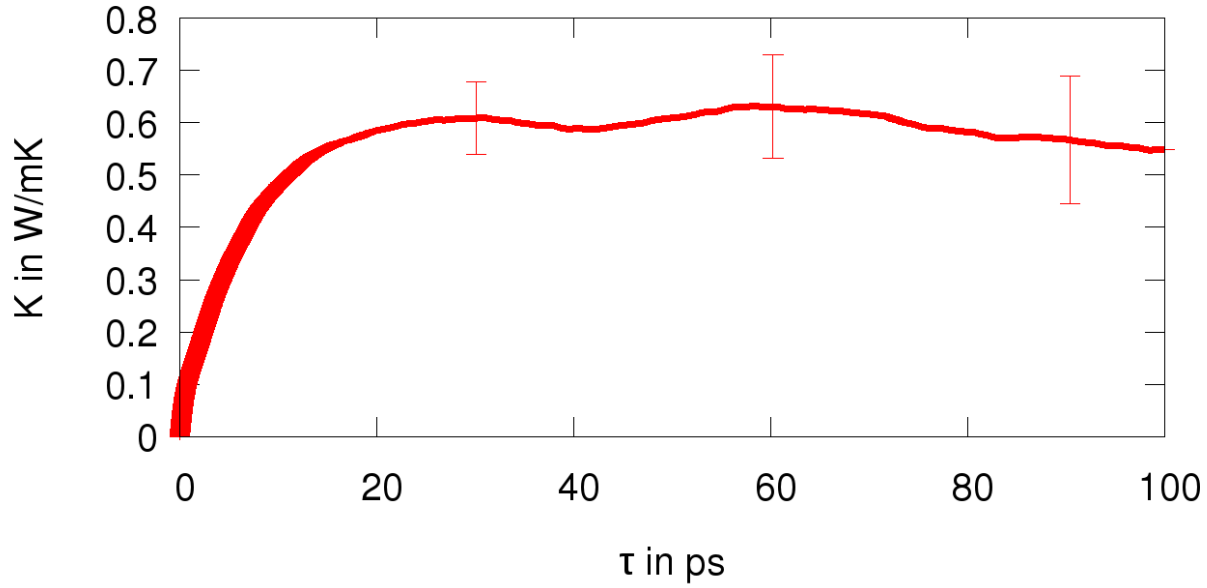

Figure 3: Real part of $\frac{\Omega}{k_B T^2} \int_0^\tau < J(0,\tau)J(0,0) > d\tau$ vs. τ graph. This is for T=20K and convergence is achieved by 20 ps.

We then plot $\left(\frac{\Omega}{k_B T^2}\right) \int_0^\infty \langle \tilde{J}_\mu(\vec{k},\tau)\tilde{J}_\nu(-\vec{k},0)\rangle d\tau$ shown in Eq. 22 for $k=0, k=\frac{2\pi}{L}$ in Fig. 4. Note, these conductivities have the expected trend that at $k=0$ and $k=\frac{2\pi}{L}$ they decrease with increasing temperature. It is also evident in the figure that the response at $k=\frac{2\pi}{L}$ is strictly less than the bulk value, which is expected since even in the ballistic regime where

the bulk thermal conductivity should be dominant. Additionally, the lower response values at $k \neq 0$ are consistent with the results of Allen [2] shown in Fig. 2.

What we found for $\tilde{K}(\frac{2\pi}{L}, \tau)$, are properties which, we will demonstrate, contain ballistic behavior. Fig.5 shows the real part of $\tilde{K}(\frac{2\pi}{L}, \tau)$ for $T = 10K, 30K, 60K$. Notice that as temperature increases the convergence time decreases. This signifies that as the temperature of the system increases the ballistic phonons have shorter lifetimes.

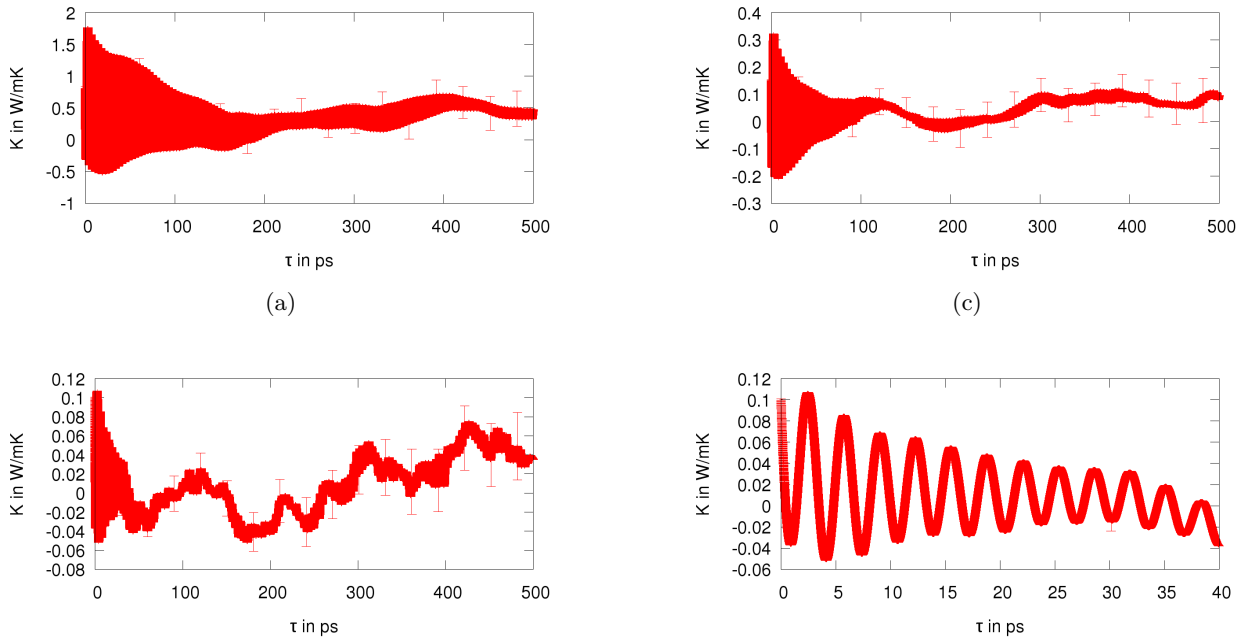

Figure 5: Real components of $\tilde{K}(\frac{2\pi}{L}, \tau)$ at T=10K, 30K, 60K. Temperatures increase from left to right with (a) 10K, (c) 30K, (b) 60K. Plot (d) is a zoomed in graph to display the sinusoidal behavior of $\tilde{K}(\frac{2\pi}{L}, \tau)$.

We then turn to Eq. 26 and examine how frequency affects the response, $\tilde{K}(\vec{k}, \tau)$ in our nonlocal model. Figs. 6 show the real and imaginary components, respectively, of $D(k, \omega)$ from Eq. 26 at different temperatures. Interestingly, there are peaks away from $\omega = 0$. Specifically, at $f = \frac{\omega}{2\pi} = 0.28THz$ there's a peak for all temperatures in the real and imaginary components of $D(\frac{2\pi}{L}, \omega)$. Fig. 8 Shows these peaks at several temperatures for both real and imaginary components. This peak is indicative of ballistic transport and shows that the system will have a stark reaction when probed near this frequency. Additionally, these peaks smear out as the temperature is increased, approaching the diffusive regime at

high temperatures. It is also important to note that as temperature increases, the magnitude of $\Re D(\vec{k},\omega)$ decreases, indicating diminishing ballistic effects. Figs 6 also demonstrate the adherence of $D(\omega,\vec{k})$ to the expected parity for both real and imaginary components.

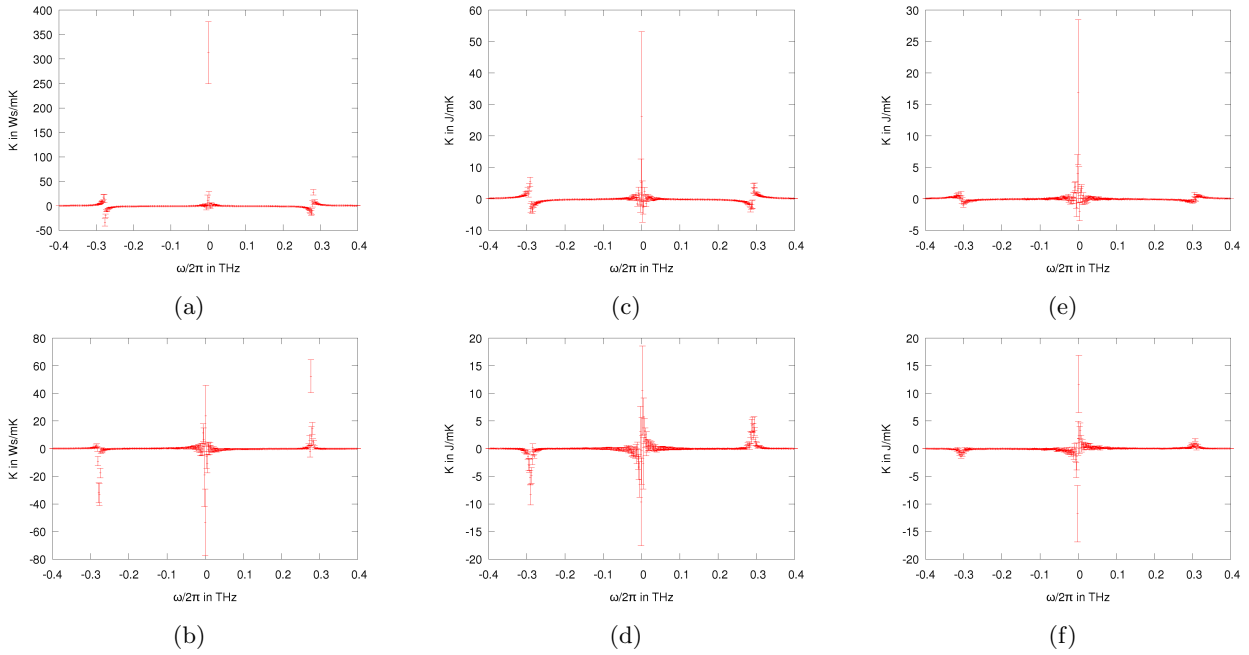

Figure 6: Real and imaginary components of $D(\frac{2\pi}{L},\omega)$ at T=10K,30K,60K. Real component is on the top, imaginary is on the bottom, temperatures increase from left to right with (a) 10K and (e) 60K.

It is instructive to compare to the Fourier theory 29, whose prediction has been plotted in Fig. 7. We compare Fig. 7 to the plots of $D(\omega,\vec{k})$ (at $\frac{2\pi}{L}$) in Fig. 6. Fig. 6 shows that the shape of $D(\omega,\vec{k})$ is congruent with that of $K_T(k,\omega)$ near $\omega = 0$. Fig 7 also reinforces our idea that the peaks from Figs 6 and 8 indeed indicate ballistic transport.

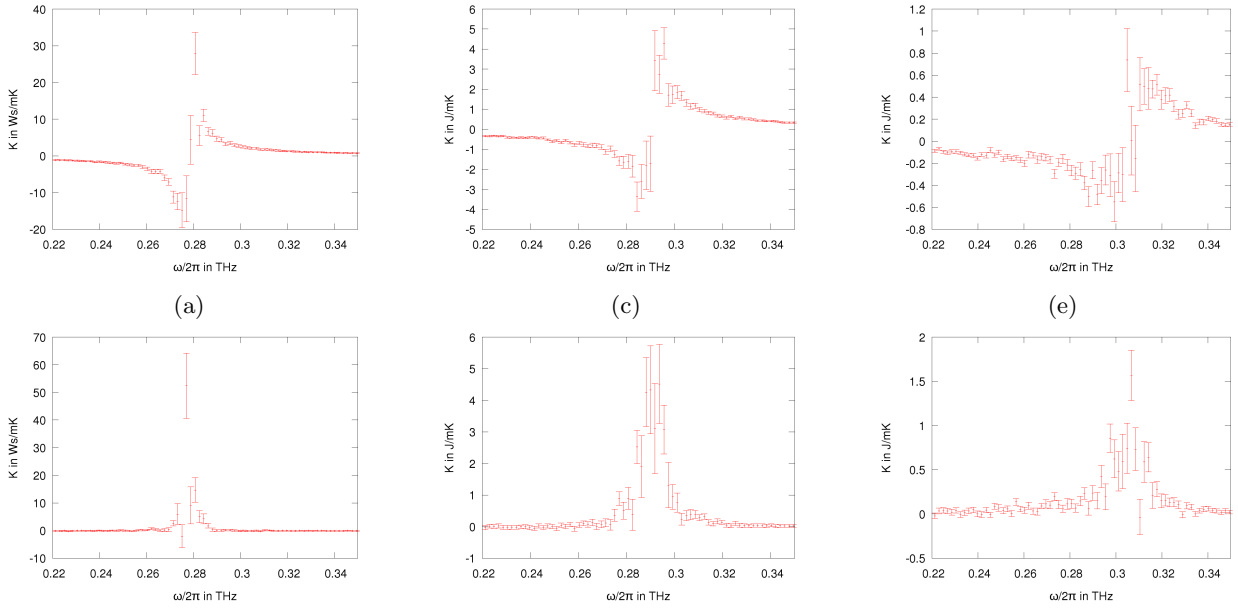

Figure 8: Real and imaginary components of $D(\frac{2\pi}{L},\omega)$ at T=10K, 30K, 60K for frequencies near outlying peaks on the positive frequency axis. Temperatures increase from left to right (a),(b) are 10K, (e),(f) are 60K The real components are on the top and imaginary components on the bottom.

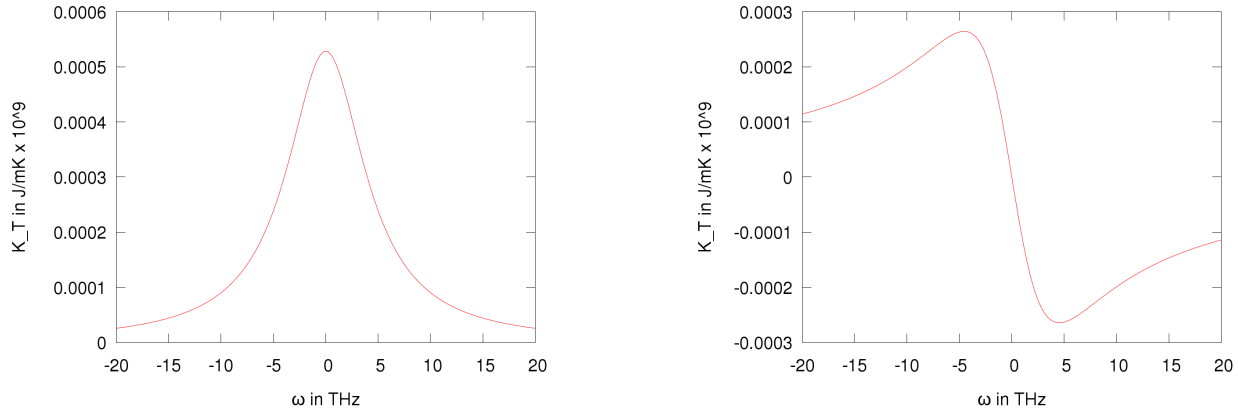

Figure 7: Real and imaginary components of $K_T(\frac{2\pi}{L},\omega)$ at T=10K; (a) real, (b) imaginary.

Suspecting that the heat carriers in this system are acoustic phonons, the speed of sound, v_s, was calculated. Since the speed of sound can be obtained from the bulk modulus, B, by $v_s = \sqrt{\frac{B}{\rho}}$ where ρ is the density of solid argon, an energy vs. volume curve fit was conducted yielding a bulk modulus of approximately 2.21 GPa. We are then able to calculate the density to be 1793.88 $\frac{kg}{m^3}$ which gives a speed of sound $v_s = 1109.93\ ms^{-1}$ using $\lambda_{mfp} = \frac{3K}{Cv}$

where $C = \frac{3Nk_B}{V_{system}}$ we obtain $\lambda_{mfp} = 3.86 \times 10^{-9}$m as the mean free path and a lifetime of $\tau_p = 3.48$ps, at T=10K. We then calculated the speed of the objects observed in the figures already shown. We find the velocity of these objects to be $v = \frac{\omega}{k} = Lf = 1208.9ms^{-1}$, coinciding with the velocity of sound, suggesting they are acoustic phonons.

We find it important to compare length scales with the data we collected. It is estimated that the width of the peak near $f = 0.28THz$ at T=10K is $\Delta f = 0.035THz$. Using the uncertainty relation $\Delta f \Delta\tau \sim 1$ we calculate $\Delta\tau \sim 28.5ps$. This timescale corresponds to a scattering time and is quite different than the phonon lifetime, τ_p, we calculated. We aren't sure of the origin of this discrepancy, a possible explanation lies in the diffusive theory's assumption that there is only one lifetime, rather than different ones for each phonon mode. The discrepancy with the convergence times in Fig. 5 is less, and could be due to not having enough MD data or our method for computing Δf.

10 CONCLUSION

We have successfully observed ballistic transport in a Lennard-Jones solid by developing and using a nonlocal Green-Kubo formalism. By considering a general nonlocal form of the current, we found the response function for a delta function external heat input. MD simulations of solid Ar using a Lennard Jones potential were conducted and wave vector, $\vec{k}$, Responses were calculated. Furthermore, we have demonstrated that the response function for an external perturbation which admits linear response has sinusoidal behavior at $\vec{k} \neq 0$ and we've successfully been able to compute responses for these Fourier modes.

By, then, exploring the Fourier transform of the $\vec{k}$ dependent thermal conductivity we have discovered peaks away from $\omega = 0$ which aren't present in the diffusive theory. We show that these peaks represent acoustic phonon modes and that a smearing effect appears as temperature is increased, demonstrating expected behavior if our formalism is to reduce to the diffusive one at high temperature and large system size. Although further investigation is required, we suspect this peak frequency will act as a resonance and may produce drastic behavior in the system response.

Although experimental verification may be difficult, we wish to apply our formalism to understand preexisting data. The nonlocal theory is typically done with the Boltzmann Transport Equation, but hasn't been done using nonlocal GK methods so we would like to apply it to understand nonlocal effects. Specifically, we would like to reproduce the results of [8] and probe systems for which the size of the heat source is not significantly larger than the mean-free paths of the heat carriers.

11 REFERENCES

References

[1] R. E. Jones A Greenstein P.K. Schelling X. W. Zhou, S. Aubry. Towards more accurate molecular dynamics calculation of thermal conductivity: Case study of gan bulk crystals. *Physical Review B*, 79, 2009.

[2] Phillip B. Allen. Analysis of nonlocal phonon thermal conductivity simulations showing the ballistic to diffusive crossover. *Physical Review B*, 97, 2018.

[3] R. Kubo. The fluctuation-dissipation theorem. *Reports on Progress in Physics*, 29:256–258, 1966.

[4] Ryogo Kubo. Statistical-mechanical theory of irreversible processes. i. general theory and simple applications to magnetic and conduction problems. *Journal of the Physical Society of Japan*, 12, 1957.

[5] P. Keblinski P. Schelling, S. Phillipot. Comparison of atomic-level simulation methods for comupting thermal conductivity. *Physical Review B.*, 65, 2002.

[6] David G. Cahill Yee Kan Koh. Frequency dependence of the thermal conductivity of semiconductor alloys. *Physical Review B*, 76, 2007.

[7] Sandro Scandolo Konstantin V. Tetriakov. Thermal conductivity of solid argon from molecular dynamics simulations. *Journal of Chemical Physics*, 120, 2004.

[8] Bo Sun Yee Kan Koh, David G. Cahill. Nonlocal theory for heat transport at high frequencies. *Physical Review B*, 90, 2014.